Ubiquinone Binding, Ubiquinone Exclusion, and Detailed Cofactor Conformation in a Mutant Bacterial Reaction Center†

Katherine E. McAuley,[§,||,○] Paul K. Fyfe,[⊥] Justin P. Ridge,[‡,#] Richard J. Cogdell,[§] Neil W. Isaacs,[||] and Michael R. Jones*[,⊥]

Division of Biochemistry and Molecular Biology and Department of Chemistry, University of Glasgow, Glasgow, G12 8QQ, U.K., Department of Molecular Biology and Biotechnology, University of Sheffield, Western Bank, Sheffield, S10 2UH, U.K., and Department of Biochemistry, School of Medical Sciences, University of Bristol, University Walk, Bristol, BS8 1TD, U.K.

Received March 10, 2000; Revised Manuscript Received June 27, 2000

ABSTRACT: The X-ray crystal structure of a *Rhodobacter sphaeroides* reaction center with the mutation Ala M260 to Trp (AM260W) has been determined. Diffraction data were collected that were 97.6% complete between 30.0 and 2.1 Å resolution. The electron density maps confirm the conclusions of a previous spectroscopic study, that the Q_A ubiquinone is absent from the AM260W reaction center (Ridge, J. P., van Brederode, M. E., Goodwin, M. G., van Grondelle, R., and Jones, M. R. (1999) *Photosynthesis Res. 59*, 9−26). Exclusion of the Q_A ubiquinone caused by the AM260W mutation is accompanied by a change in the packing of amino acids in the vicinity of the Q_A site that form part of a loop that connects the DE and E helices of the M subunit. This repacking minimizes the volume of the cavity that results from the exclusion of the Q_A ubiquinone, and further space is taken up by a feature in the electron density maps that has been modeled as a chloride ion. An unexpected finding is that the occupancy of the Q_B site by ubiquinone appears to be high in the AM260W crystals, and as a result the position of the Q_B ubiquinone is well-defined. The high quality of the electron density maps also reveals more precise information on the detailed conformation of the reaction center carotenoid, and we discuss the possibility of a bonding interaction between the methoxy group of the carotenoid and residue Trp M75. The conformation of the 2-acetyl carbonyl group in each of the reaction center bacteriochlorins is also discussed.

The bacterial reaction center is a membrane-bound pigment−protein complex that catalyzes the transduction of light energy into electrochemical potential energy. In *Rhodobacter* (*Rb.*)[1] *sphaeroides*, the reaction center has three subunits, two of which, termed L and M, each have five transmembrane α-helices and are arranged around an axis of 2-fold symmetry that runs approximately perpendicular to the plane of the bacterial inner membrane (*1*−*5*). The L and M subunits encase four molecules of bacteriochlorophyll (BChl), two molecules of bacteriopheophytin (BPhe), two molecules of ubiquinone-10 (UQ_{10}), a carotenoid, and a non-heme iron. The BChl, BPhe, and UQ_{10} cofactors are arranged in two branches that span the membrane. In the initial photochemical reaction, light energy is used to drive the transfer of an electron from an excitonically coupled pair of BChl molecules (P), which straddle the symmetry axis close to the periplasmic side of the membrane, to a UQ_{10} (Q_A) located close to the cytoplasmic side (*6*, *7*). This electron transfer takes place in approximately 200 ps and involves, as intermediate electron carriers, a monomeric BChl (B_L) and a BPhe (H_L). The remaining monomeric BChl and BPhe (B_M and H_M) on the symmetry-related cofactor branch do not participate in transmembrane electron transfer, but the B_M BChl is involved in the transfer of triplet energy to the single carotenoid of the reaction center (*8*−*10*). This carotenoid, which is spheroidenone in *Rb. sphaeroides* reaction centers isolated from cells grown under semiaerobic conditions, fulfils a photoprotective function, dissipating the energy of BChl triplet states before they can react to form singlet oxygen (*8*−*10*).

Research on the bacterial reaction center has been greatly aided by the determination of X-ray crystal structures for the complex from *Rhodopseudomonas* (*Rps.*) *viridis* (*11*, *12*) and *Rb. sphaeroides* (*1*−*5*, *13*), and in particular these structures have guided the application of site-directed mutagenesis. In recent years, a combination of mutagenesis and spectroscopy has been used to investigate how the protein modulates the biophysical properties of the reaction center cofactors and to investigate the mechanism of light-driven electron transfer and associated protonation reactions (*14*−*17*). Directed mutagenesis has also been used to alter the cofactor composition of the reaction center, most notably

† This work was supported by the Biotechnology and Biological Sciences Research Council of the United Kingdom and Wellcome Trust Grant 043492.

* Corresponding author. Telephone: 44-117-9287571. Fax: 44-117-9288274. E-mail: m.r.jones@bristol.ac.uk.

‡ University of Sheffield.

§ Division of Biochemistry and Molecular Biology, University of Glasgow.

|| Department of Chemistry, University of Glasgow.

⊥ University of Bristol.

Present address: Department of Microbiology, University of Queensland, St. Lucia, Brisbane, QLD 4072, Australia.

○ Present address: Department of Chemistry, University of York, Heslington, York, YO10 5DD, United Kingdom.

[1] Abbreviations: BChl, bacteriochlorophyll; BPhe, bacteriopheophytin; LDAO, lauryldimethylamine oxide; P, primary donor; *Rb*, *Rhodobacter*; *Rps. Rhodopseudomonas*.

10.1021/bi000557r CCC: $19.00
Published on Web 11/10/2000

through the replacement of BChl by BPhe, or vice versa, or the exclusion of individual cofactors (*14*−*17*).

In a recent report, the spectroscopic properties of a reaction center with the mutation Ala M260 to Trp (AM260W) were described (*18*). This reaction center was not capable of supporting photosynthetic growth of *Rb. sphaeroides* and appeared to lack a functional Q_A ubiquinone, as a result of which light-driven electron transfer was blocked at the H_L BPhe. The kinetics of primary electron transfer from P to H_L were not affected by the AM260W mutation (*18*).

In this report, we describe an X-ray crystal structure for the AM260W reaction center, derived from diffraction data that were 97.6% complete between 30.0 and 2.1 Å resolution. The electron density maps confirm that the Q_A ubiquinone is absent from the AM260W reaction center and show that there is a change in the packing of amino acids in the vicinity of the Q_A site to minimize the volume of the cavity that results from the exclusion of this cofactor. The occupancy of the Q_B sites appears to be high in the AM260W crystals, and the position of the Q_B ubiquinone is well-defined. The high quality of the electron density maps also reveals more precise information on the detailed conformation of the reaction center carotenoid and bacteriochlorin cofactors. The coordinates of the structure of the AM260W reaction center have been deposited in the Protein Data Bank under accession code 1QOV. Crystallographic information on the binding of the diacidic phospholipid cardiolipin to the intramembrane surface of the AM260W reaction center has been described in a recent publication (*19*), and the present report presents a more detailed description of the structure of this mutant reaction center.

MATERIALS AND METHODS

Mutagenesis. The mutation Ala M260 to Trp (AM260W) was introduced into the *pufM* gene of the reaction center using a mismatch oligonucleotide as described in detail in a recent publication (*18*). The mutated *pufM* gene was expressed in the double deletion/insertion mutant strain DD13, as described in detail previously (*20*, *21*). The resulting strain, named AM260W, lacked both the LH1 and LH2 antenna complexes and contained the mutant reaction center as the sole pigment−protein complex.

Cell Growth and Purification of Reaction Centers. Rb. sphaeroides strain AM260W was grown under semiaerobic/dark conditions at 34 °C in M22+ medium, and intracytoplasmic membranes were isolated by breakage of harvested cells in a French pressure cell, as described previously (*22*, *23*). Membranes were pelleted by ultracentrifugation at ∼250000*g* for 1.5 h and were resuspended to a concentration of approximately 10 AU cm^{-1} at 800 nm in 20 mM Tris/HCl (pH 8.0).

Reaction centers were isolated by exposure of resuspended membranes to the detergent lauryldimethylamine oxide (LDAO), as described in a recent publication (*23*). Purification of the reaction centers was achieved by two passes of the solubilized material through a DE52 (Whatman) anion exchange column, followed by further anion exchange separation on a Sepharose Q column (Pharmacia) and gel filtration using a Superdex200 preparative grade column (Pharmacia), as described in detail elsewhere (*23*). After the final chromatography step, pooled reaction centers typically had an absorbance ratio $A_{280}/A_{800} = 1.3$ and were suitable for crystallization.

Purified reaction centers were concentrated in a stirred ultrafiltration cell (Amicon) under nitrogen gas, followed by further concentration in Centricon concentrators (Amicon). The reaction centers were then washed with 10 mM Tris/HCl (pH 8.0)/0.1% LDAO and were reconcentrated using Centricon concentrators. This washing was repeated at least five times to ensure good buffer exchange, and the reaction centers were brought to a final concentration of 60 AU cm^{-1} at 800 nm, again in 10 mM Tris/HCl (pH 8.0)/0.1% LDAO.

Crystallization of Reaction Centers. Trigonal crystals (*24*), space group $P3_121$, were grown by sitting drop vapor diffusion from droplets containing 10 mg/mL of reaction center, 0.1% v/v LDAO, 3.5% w/v 1,2,3-heptanetriol, 0.5 M trisodium citrate, and 10 mM Tris/HCl (pH 8.0). The drops were equilibrated against a reservoir of 1.1 M trisodium citrate. Trigonal crystals appeared within 1−4 weeks and ranged from 0.5 to 1.5 mm in the longest dimension. The crystals had unit cell dimensions of $a = b = 142.0$ Å, $c = 186.8$ Å.

Data Collection and Analysis. X-ray diffraction data were collected at room temperature at beam line 9.6 of the Daresbury Synchrotron Radiation Facility, using a Quantum-4 ADSC detector, and were processed using the Denzo and Scalepack packages (*25*). Data collection and refinement statistics are shown in Table 1. A total of 124 853 unique reflections were recorded using two crystals, giving data that were 97.6% complete between 30.0 and 2.1 Å and 82.9% complete in the outer shell (2.15−2.1 Å), with an overall multiplicity of 4.2 and an overall R_{merge} of 5.7%. The R_{merge} for the outer shell was 28.1%. Rigid body refinement was performed using XPLOR 3.1 (*26*) using the coordinates of the wild-type reaction center from the antenna-deficient strain RCO2 (*23*) as a starting model, followed by restrained maximum likelihood refinement in REFMAC (*27*), with waters fitted by ARPP (*28*). The restraints used during refinement were as follows: The restraints of Engh and Huber were used for the protein chains of the complex (*29*). The restraints for the reaction center cofactors were based on XPLOR parameter and topology files used in a previous publication (*23*), which were a gift from Ulrich Ermler, Günter Fritzsch, and Roy Lancaster. The information in these files was used to create dictionaries for the cofactors in PROTIN format, and a new dictionary was made for cardiolipin. The ideal geometry values for the lipid and carotenoid were obtained from analysis of the Cambridge Structural Database (*30*). Figures were produced using the programs Molscript (*31*), Raster3D (*32*), and XtalView (*33*).

RESULTS

X-ray Crystallography. Reaction centers containing the AM260W mutation were purified and crystallized as described in brief in Materials and Methods, using a protocol described in detail in a previous publication (*23*). The only changes to the crystallization conditions in the present study were the replacement of potassium phosphate as precipitant by sodium citrate and the omission of 1,4-dioxane. After refinement, the structure of the AM260W reaction center was found to be similar to that of the wild-type reaction center (*4*, *5*, *23*), with the exception of the regions around the

Table 1: Crystallographic Statistics for Data Collection and Refinement

	AM260W reaction center
Collection Statistics	
no. of unique reflections	124 853
completeness[a]	97.6% (82.9%)
multiplicity	4.2 (1.6)
R_{merge}[a,b]	5.7% (28.1%)
Refinement Statistics	
resolution range	30.0−2.1 Å
R factor[c]	16.9%
free-*R* factor[d]	18.6%
average *B* factor	40.0 Å^2
Geometry	
rmsd from ideality	
bonds	0.011 Å
angles	0.026°
Ramachandran Plot, Residues in:[e]	
most favored areas	93.2%
additional allowed areas	6.5%
generously allowed areas	0.3%
disallowed areas	0.0%
coordinate error[f]	0.10 Å
Model	
no. of protein residues	823
no. of cofactors	4 BChl, 2 BPhe, 1 Ubi,[g] 1 Spo,[g] 1 Fe[g]
no. of waters	250
no. of detergents	0
no. of lipids	1 Cdl[g]

[a] Figures within parentheses refer to the statistics for the outer resolution shell (2.15−2.10 Å). [b] $R_{merge} = \sum_h\sum_i|\langle I(h)\rangle - I(h)_i|/\sum_h\sum_i I(h)_i$ where $I(h)$ is the intensity of reflection h, $\sum_h$ is the sum over all reflections, $\sum_i$ is the sum over all i measurements of reflection h. [c] *R* factor is defined by $\sum||F_o| - |F_c||/\sum|F_o|$. [d] Free-*R* was calculated with 5% reflections, selected randomly (*61*), and these reflections were omitted from all refinement steps. [e] Ramachandran plot was produced by Procheck version 3.0 (*62*). [f] Coordinate error was estimated by DPI (*63*). [g] Cdl = cardiolipin (diphosphatidyl glycerol); Fe = non-heme iron; Spo = spheroidenone; Ubi = ubiquinone.

ubiquinone binding pockets that are described in detail below. Superimposition of the α-carbons of the structures of the wild-type (*4*, *5*, *23*) and AM260W reaction centers using the program LSQKAB (*34*) gave a root-mean-square displacement of 0.291 Å. Those regions of the protein not resolved in data on the wild-type reaction center (*4*, *5*, *23*) were also disordered in the map of the AM260W reaction center. These were the first 10 amino acids of the H chain, residues 251−260 of the C terminus of the H chain, and residues 303−307 of the C terminus of the M chain. The structural model of the AM260W reaction center included a molecule of cardiolipin; the structural details of this lipid and the manner in which it binds to the intramembrane surface of the reaction center have been described in detail in a recent publication (*19*).

The electron density maps obtained for the AM260W reaction center were of particularly good quality. There were several reasons for this. First, the crystals of the AM260W reaction center diffracted to high resolution, with initial diffraction being observed to 1.8 Å. In addition, data were collected with a high completeness (82.9% complete in the 2.15−2.10 Å resolution shell) for the reasons outlined below. The attainment of a high overall resolution was aided by the use of an ADSC detector, together with a particularly high beam flux, which meant that the time required for acquision of a full data set was relatively short (2 h compared with >60 h for an equivalent number of images in our previous experiments using other detectors). As a result, radiation damage of the crystals leading to loss of high-resolution diffraction was minimized. Furthermore, the precision of the measured data was greater than for other structures we have reported (*23*, *35*−*37*), again largely due to use of the ADSC detector. Finally, the relatively rapid data acquisition meant that it was possible to collect data with a high completeness and multiplicity, and the data collected included low-resolution reflections (30.0−10.0 Å), which were also used in the refinement.

Structure of the Q_A Site. In the wild-type reaction center, the Q_A site is formed by residues from the D, DE, and E helices of the M subunit and the loop connecting the DE and E helices (*38*, *39*). The distal and proximal (to the non-heme iron) carbonyl oxygens of the Q_A headgroup form hydrogen bond interactions with the backbone nitrogen of Ala M260 and the side chain of His M219, respectively (*4*, *5*). Figure 1A shows part of the electron density map and fitted structure of the wild-type RCO2 reaction center (*23*), focusing on the headgroup of the Q_A ubiquinone and surrounding residues, including Ala M260 and His M219. In the equivalent region of the AM260W reaction center (Figure 1B), the density corresponding to the Trp M260 occupied part of the volume that is normally occupied by the ubiquinone headgroup in the wild-type reaction center. The conclusion that the AM260W mutation causes exclusion of the Q_A ubiquinone, which was based on physiological and spectroscopic data, was therefore supported by the crystallographic data obtained for the AM260W reaction center, which showed no indication of binding of ubiquinone at or near the Q_A site. With one exception, detailed below, all of the electron density in the immediate vicinity of the Q_A site in the AM260W reaction center could be accounted for by the backbone and residues of the M subunit or by water molecules.

Exclusion of the Q_A ubiquinone from the AM260W reaction center left a cavity in the interior of the reaction center which was only partially filled by Trp M260. This Trp residue occupied approximately half of the volume that is occupied by the Q_A headgroup in the wild-type complex (Figure 1). The volume of the cavity created by the exclusion of the Q_A ubiquinone was further reduced by the presence of a group that gave rise to an intense spherical feature in the electron density that is shown just to the right of Trp M260 in Figure 1B. This density peak was too intense to be attributable to a water molecule, having a value of approximately 9σ, and has been attributed to an ion. An ion at this position would not only serve to fill up part of the cavity created by exclusion of the Q_A headgroup, as illustrated in Figure 1B, but could also satisfy bonding requirements of surrounding groups. The ion is located approximately 3.1 Å from the indole nitrogen of Thr M260, 3.0 Å from the ND nitrogen of His M219, and 3.5 Å from the side-chain oxygen of Met M222. The lengths of these possible bonding interactions were too great for the ion to be a metal, and the density itself was too small and spherical in nature to be attributable to a complex ion such as sulfate or phosphate. In light of this, we have modeled this feature as a chloride ion as, of the likely candidates, chloride was the most abundant ion in the growth medium. Further investigation will be required to obtain a definite identification. In addition,

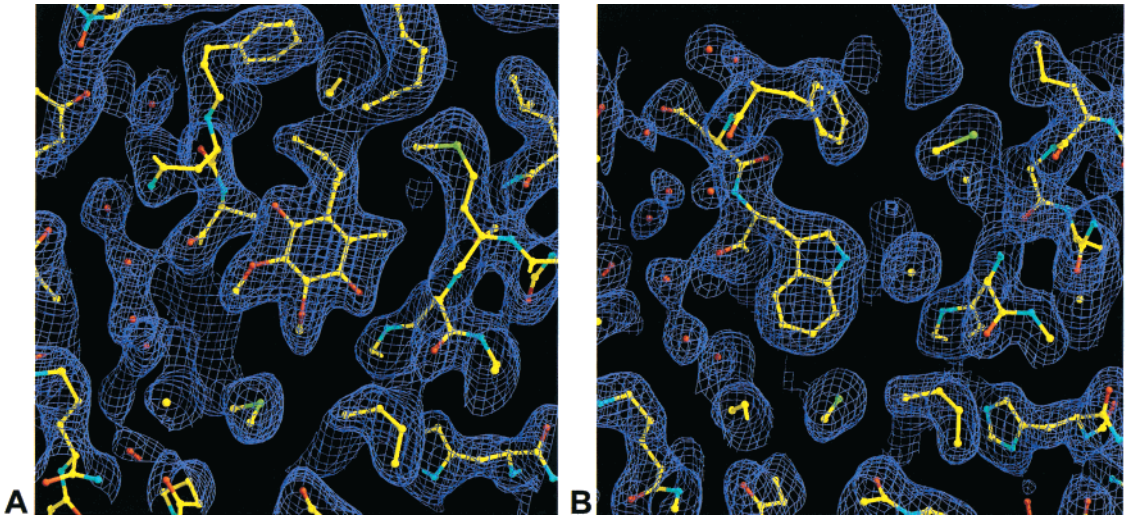

FIGURE 1: Electron density in the Q_A binding pocket. (A) REFMAC $2mF_o - DF_c$ electron density map of the RCO2 (wild-type) reaction center with the fitted structure of the Q_A ubiquinone and the surrounding protein. The view includes residues Ala M260 (to the left of the ubiquinone) and Phe M258 (top center). (B) Same view as in part A of the REFMAC $2mF_o - DF_c$ electron density map of the AM260W reaction center with the fitted structure of the protein. The view includes residue Trp M260 (center) and Phe M258 (top center).

it is not yet clear whether this ion is present at this position in AM260W reaction centers in intact cells or whether it is incorporated during reaction center purification and crystallization.

The volume of the cavity created by the exclusion of the Q_A ubiquinone was further reduced by limited repacking of residues that line the Q_A binding pocket. The structure of this pocket in the wild-type reaction center is shown in Figure 2A. Figure 2B shows a stereoview of the amino acids that line the Q_A pocket in the wild-type reaction center, while Figure 2C shows the conformation of the same amino acids in the AM260W reaction center. The repacking mainly affected residues M256−M260, which form part of a loop connecting the transmembrane E helix and DE helix of the M subunit. This loop is highlighted with an orange backbone in Figure 2. The repacking also affected residue Gln H32 (part of the H subunit is shown with a blue backbone in Figure 2), which is located close to residues Phe M258 and Asn M259. The largest change in packing was movement of residue Phe M258, which is also apparent by comparison of Figure 1B with Figure 1A. In the AM260W reaction center, this residue occupies a position that is equivalent to the position of the first two isoprenoid units of the tail of the Q_A ubiquinone in the wild-type reaction center. There was also significant movement of residues Asn M259 and Met M256 (Figure 2C), the latter also having moved toward the cavity created by exclusion of the tail of the Q_A ubiquinone. As is apparent from Figure 2, the repositioning of residues M256−M260 was accompanied by a change in the conformation of the backbone in that region of the M subunit (highlighted in orange in Figure 2). Comparison of the positions of the C_α carbons of the L, M, and H polypeptides in the structural models of the AM260W and RCO2 reaction centers using the program LSQKAB (*34*) revealed the extent of this. Superposition of the two data sets was excellent, apart from a short stretch of residues between positions M256 and M261 (see Supporting Information). Repacking of the backbone between M256 and M261 can be seen by comparing Figure 2C with Figure 2B.

The packing of residues contributed to the Q_A binding pocket by the D, DE, and E helices of the M subunit was largely unaffected by exclusion of the Q_A ubiquinone and the structural changes outlined above. In particular, residue Trp M252, which is stacked between the headgroup of the Q_A ubiquinone and the H_L BPhe, was not affected by the structural changes (Figure 2). A small change in the angle of residue His M219 was observed (approximately 15°), reflecting the fact that this residue was no longer interacting with the proximal carbonyl group of the Q_A headgroup but was probably interacting with the species designated as a chloride ion. This small change in packing did not have a significant effect on the interaction of this residue with the non-heme iron (see below). The possible interactions of the chloride ion with Trp M260 and His M219 are also apparent in Figure 2C.

Effects of Protein Repacking near the Q_A Site on the Remainder of the Protein. With the exception of the changes detailed above, the mutation at the M260 position had no significant effect on the structure of the reaction center (bearing in mind that the estimated coordinate error for the structures discussed in this report is of the order of 0.1 Å). In particular, there was no change in the conformation of the residues that form the binding pocket of the Q_B ubiquinone and the structure of the non-heme iron and surrounding ligands was also not affected, with the exception of the slight change in conformation of His M219 mentioned above. To quantitate this, the bond lengths between the non-heme iron and the six surrounding ligands were compared in the structures of the AM260W and RCO2 (wild-type) reaction centers. These bond lengths did not vary by more than 0.3 Å when the structures were compared, and most were conserved to within 0.1 Å. There were also no significant changes in structure in the vicinity of the reaction center BChls and BPhes, consistent with the conclusion derived from spectroscopic data that the mutation had very little effect on the absorbance properties of these cofactors, and no discernible effect on the rate of primary electron transfer (*18*).

Although no significant changes in structure outside the immediate vicinity of the Q_A site were apparent, the excellent quality of the electron density maps obtained for the AM260W reaction center did bring some additional insights

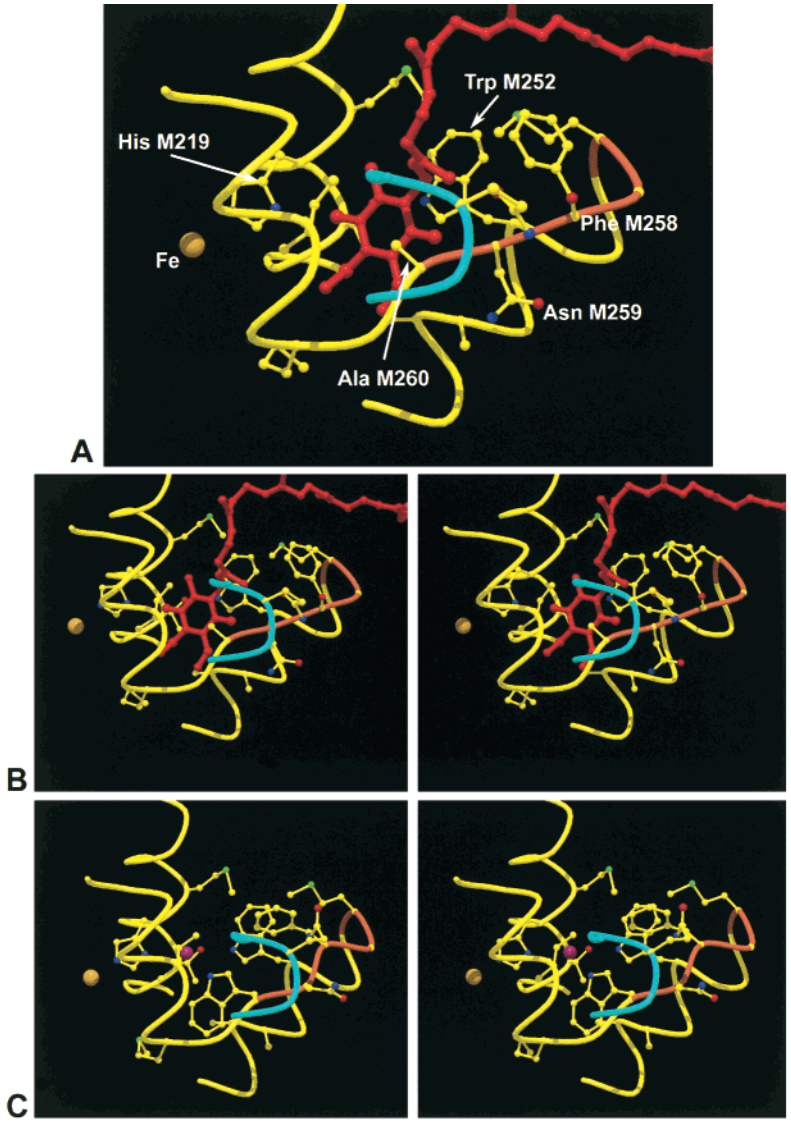

FIGURE 2: Structural models of the Q_A binding pocket. (A) The binding pocket of the Q_A ubiquinone (red) in the RCO2 (wild-type) reaction center, consisting of stretches of the D, DE, and E helices of the M subunit (yellow backbone), the loop connecting the DE and E helices (orange backbone), the A helix of the H subunit (cyan backbone), and the non-heme iron (brown sphere). Fourteen amino acid residues are shown, and the residues mentioned in the text are labeled. (B) Stereoview of the model of the RCO2 (wild-type) reaction center. (C) Stereoview of the model of the AM260W reaction center, showing the Trp M260 residue, the repacking of residues in the loop (residues M256−M260) connecting the DE and E helices (orange backbone), and the chloride ion (purple sphere).

into a number of aspects of the detailed structure of the reaction center cofactors, which are discussed below.

Structure of the Q_B Site. In contrast to the Q_A site in the wild-type reaction center, where ubiquinone forms an integral part of the complex, ubiquinone binding at the Q_B site is transient and the ubiquinone may be lost during purification of the complex. A feature of the data typically collected for both the *Rb. sphaeroides* and *Rps. viridis* reaction centers is that the electron density attributable to the native Q_B ubiquinone is poorly defined compared to that of the surrounding protein and the other reaction center cofactors. This poor definition appears to be due to a low occupancy of the Q_B site by ubiquinone and the possibility of more than one binding conformation for the Q_B ubiquinone, with accompanying changes in the number and position of crystallographically defined water molecules (*40*, *41*). The first description of the trigonal crystal form of the wild-type *Rb. sphaeroides* reaction center reported a high-temperature factor for the Q_B ubiquinone relative to that of the surrounding protein, indicating that the occupancy of the Q_B site was rather low (*4*, *5*). Our own findings on the wild-type reaction center and a number of mutant complexes agree with this observation (unpublished data), and a similar low occupancy of the Q_B site has been reported for the *Rps. viridis* reaction center (*12*).

When the diffraction data for the AM260W reaction center were examined, it was apparent that the electron density attributable to the Q_B ubiquinone was unusually well-defined. To illustrate this, in Figure 3, an electron density map for the AM260W reaction center in the region of the Q_B site (Figure 3B) is compared with a map of the same region from data collected at 2.3 Å resolution for a WM115F/FM197R mutant reaction center (Figure 3A) (*35*), which represents our "next best" structure in terms of resolution (the WM115F and FM197R mutations do not affect the structure of the Q_B site). In the context of Q_B site structure, the data obtained for the WM115F/FM197R reaction center is typical of that obtained in our studies (seven structures determined to date

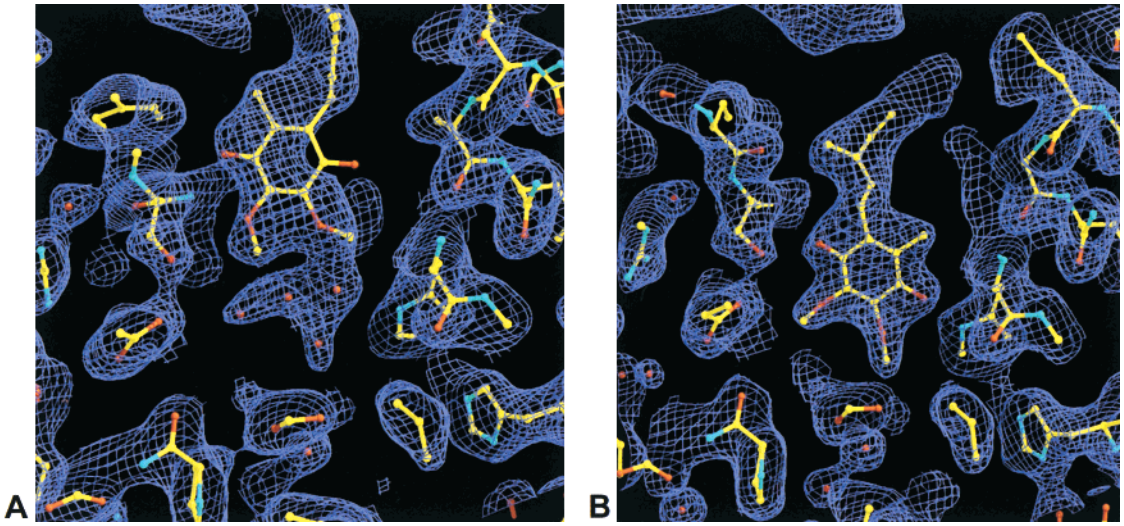

FIGURE 3: Electron density in the Q_B binding pocket. (A) REFMAC $2mF_o - DF_c$ electron density map of the WM115F/FM197R reaction center (PDB entry 1E6D) with the fitted structure of the Q_B ubiquinone, four adjacent water molecules, and the surrounding protein. (B) Same view as in part A of the REFMAC $2mF_o - DF_c$ electron density map of the AM260W reaction center, with the fitted structure of the Q_B ubiquinone and the surrounding protein.

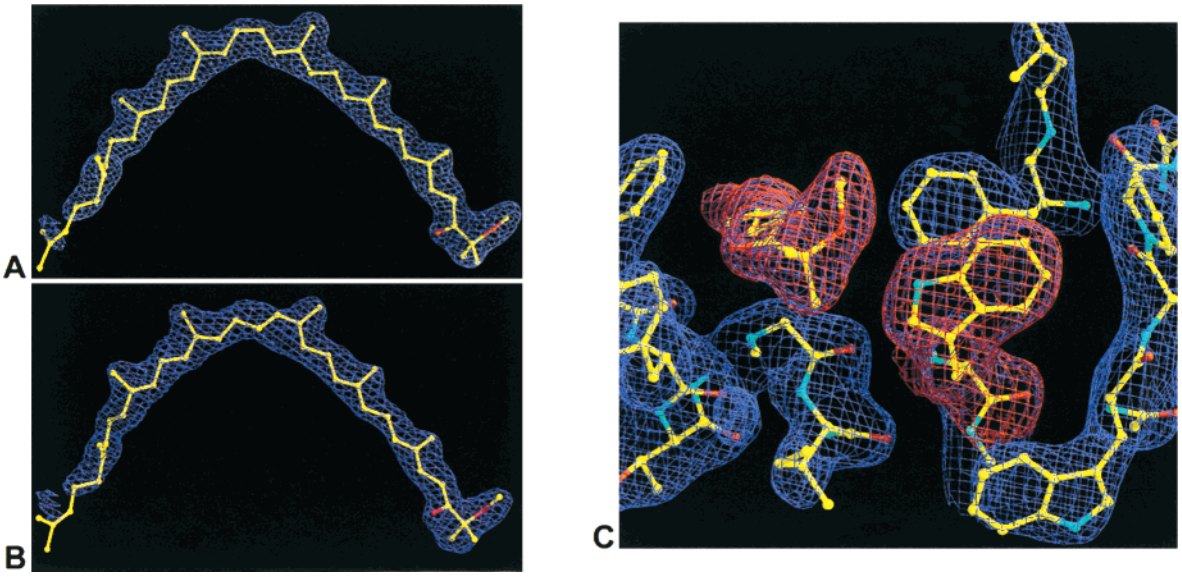

FIGURE 4: Electron density attributable to the reaction center carotenoid in the AM260W reaction center. (A,B) REFMAC $2mF_o - DF_c$ electron density map of the reaction center carotenoid with the fitted structure of spheroidenone in (A) the 15,15′ cis conformation and (B) the 13,14-cis conformation. (B) REFMAC $2mF_o - DF_c$ electron density map of the methoxy end of the reaction center carotenoid and density attributed to neighboring amino acids. Electron density attributable to the carotenoid and residue Trp M75 is highlighted in red.

for wild-type or mutant reaction centers at resolutions of between 2.8 and 2.3 Å). The coordinates of the structure of the WM115F/FM197R reaction center have been deposited with the Protein Structure Databank, under entry 1E6D. As shown in Figure 3A, the electron density data for the WM115F/FM197R reaction center did not clearly define the position of the Q_B ubiquinone. The headgroup of the ubiquinone was modeled in the region of highest density, and four water molecules were modeled into the remaining density located deeper in the pocket. In marked contrast, in the data obtained for the AM260W reaction center, the position of the Q_B ubiquinone was clearly defined (Figure 3B). The O4 carbonyl oxygen of the Q_B ubiquinone was within hydrogen bond distance of His L190 (2.6 Å), and the O1 carbonyl oxygen was within hydrogen bond distance of the backbone amide nitrogen of Ile L224 (3.0 Å) and within 2.7 Å of the side-chain oxygen of Ser L223 (2.7 Å).

The well-defined electron density for the Q_B ubiquinone suggested that the occupancy of the Q_B binding pocket was significantly greater that that routinely observed for this crystal form of the reaction center, and possible reasons for this are considered in the Discussion. The mean temperature factor for the atoms of the headgroup of the Q_B ubiquinone in the AM260W reaction center was calculated to be 47.6 $Å^2$, compared with a value of 31.0 $Å^2$ for a selection of 10 residues (including main chain atoms) in the immediate vicinity of the Q_B ubiquinone. This would indicate an occupancy of at least 65% of the Q_B sites in the AM260W crystals.

Conformation of Spheroidenone. In Figure 4 we show the electron density attributable to the reaction center carotenoid, which was spheroidenone in the present study and a fit to this density of 15,15′-cis and 13,14-cis structures for spheroidenone (parts A and B of Figure 4, respectively). In

previous reports on the structure of carotenoid-containing *Rb. sphaeroides* reaction centers (*4*, *5*, *42*−*45*), it has not been possible to discriminate conclusively between these two possible conformations for the reaction center carotenoid, and previous data collected by us for both wild-type and mutant reaction centers have also been ambiguous on this point (not shown). The higher quality maps obtained with the AM260W reaction center clearly show that a 15,15′-cis arrangement gives a better fit to the electron density in omit maps, in full agreement with long-standing conclusions based on NMR and Raman spectroscopy (*46*, *47*). Similar results have been obtained for 1,2-dihydroneurosporene in the *Rps. viridis* reaction center (*48*).

A feature of the binding of spheroidene/spheroidenone by the *Rb. sphaeroides* reaction center is that no bonding interactions have been identified between the carotenoid and the surrounding protein. In addition to improved detail on the conformation of the spheroidenone, the data collected for the AM260W reaction center revealed a possible hydrogen bond interaction between residue Trp M75 and the terminal methoxy group of the spheroidenone (Figure 4C). In the structural model of the AM260W reaction center, the best fit to the electron density was obtained with the side-chain nitrogen of Trp M75 pointing toward the methoxy oxygen of the carotenoid (Figure 4C). In this conformation, the separation of the nitrogen and oxygen was 3.1 Å, suggesting a possible hydrogen bond interaction between the two. Possible implications of this interaction are considered below. The keto oxygen of the spheroidenone does not form a hydrogen bond interaction with the surrounding protein.

Orientation of the Acetyl Groups of the Reaction Center Bacteriochlorins. Each of the reaction center BChls and BPhes has an acetyl carbonyl group attached to carbon 2 of ring I. This carbonyl group is conjugated to the π electron system of the bacteriochlorin and provides a point at which the protein can make a through-bond connection with the bacteriochlorin macrocycle. The angle that the 2-acetyl carbonyl group makes with the plane of the bacteriochlorin ring is thought to be important, as this is expected to affect the strength of the conjugation of the carbonyl group with the remainder of the π electron system (*49*). The strength of this conjugation should decrease as the carbonyl group is rotated out of the plane of the bacteriochlorin macrocycle. Examination of the structures of the *Rb. sphaeroides* reaction center available in the Protein Data Bank shows some variation in the modeled orientation of the 2-acetyl carbonyl group, relative to the plane of the bacteriochlorin ring, for each of the reaction center BChls and BPhes. An additional complication is that, at the resolutions of the available structures, it is not possible to assign the oxygen and methyl "arms" of the 2-acetyl carbonyl groups. As a result, the assignments made in the available structures should be regarded with caution.

With the good quality electron density maps obtained for the AM260W reaction center, we examined the orientations of the 2-acetyl carbonyl groups. To evaluate the orientation of the acetyl groups of the six reaction center bacteriochlorins, refinements were performed in REFMAC (*34*) with the acetyl groups at the orientations previously assigned in the structural model of the wild-type reaction center or with all of the acetyl groups rotated by 180 degrees relative to these orientations. The most likely orientation for each bacteriochlorin was assigned on the basis of these refinements. Two further rounds of refinement were then performed, one using these assignments and one with all of the acetyl groups rotated by 180° (alternative conformation). This second round of refinements gave a difference in *R* factor of 0.03% and a difference in free *R* of 0.1%, in both cases favoring the assigned conformations over the alternative conformations.

Figure 5A shows a fit of the structure of the P_L BChl to the electron density to illustrate the quality of the data. A view of the orientation of the 2-acetyl carbonyl group relative to the plane of the macrocycle for each of the reaction center BChls and BPhes is shown in Figure 5B−G. In some cases it was clear that one of the two possible gross orientations provided a better fit to the data, reflecting an apparent asymmetry in the electron density of the acetyl group which is evident in the example shown in Figure 5A. However, this discrimination was clearer in some cases than in others, and to err on the side of caution given the resolution of the data obtained in the present study, we have concluded that it is not possible to *unequivocally* assign the methyl and oxygen arms of the group. The fits shown in Figure 5B−G should therefore be regarded as the most likely assignments, made on the basis of the available data, rather than definitive statements of the correct assignment.

The orientation of the 2-acetyl carbonyl group is often discussed in terms of the C12−C2−C2a−O dihedral angle ϕ_{Ac}. Figure 5B−G shows edge-on views of the 2-acetyl carbonyl groups, viewed down the axis of the C2−C2a bond with the horizontal axis being defined by the C12−C2 bond of ring I. The 2-acetyl carbonyl of B_M (Figure 5B) is oriented nearly in the plane of the macrocycle, with $\phi_{Ac} = 350°$ (or $-10°$), while the group of B_L lies more out-of-plane, with $\phi_{Ac} = 333°$ (or $-27°$) (Figure 5E). These groups reside in largely apolar environments and do not form hydrogen bond interactions with the surrounding protein. The 2-acetyl carbonyl of P_L has $\phi_{Ac} = 13°$ (Figure 5C) and points toward His L168 (according to the most likely assignment), with the oxygen of the carbonyl group located 3.0 Å from the NE2 nitrogen of His L168. The 2-acetyl carbonyl of P_M (Figure 5D) shows an approximately symmetrical arrangement to that of P_L, with $\phi_{Ac} = 5°$ and the carbonyl oxygen (probably) pointing toward Phe M197. The 2-acetyl groups of H_M (Figure 5F) and H_L (Figure 5G) both lie out of the plane of the BPhe ring, with $\phi_{Ac} = 43°$ and $\phi_{Ac} = 28°$, respectively. Neither carbonyl group is hydrogen bonded to the surrounding protein.

DISCUSSION

Ubiquinone Exclusion at the Q_A Site. The main purpose of this study was to examine the structural basis for an apparent lack of Q_A function in the AM260W mutant reaction center and to look at the extent of any structural changes caused by the mutation. The first conclusion that can be drawn from the data presented above is that the changes in the structure of the protein−cofactor complex that occur in response to the AM260W mutation are confined to the immediate vicinity of the Q_A binding pocket. This is in line with the observations of Ridge and co-workers (*18*) that there is little effect of the mutation on the absorbance spectrum of the reaction center bacteriochlorins, on the midpoint potential of the P dimer, or on the rate of primary electron

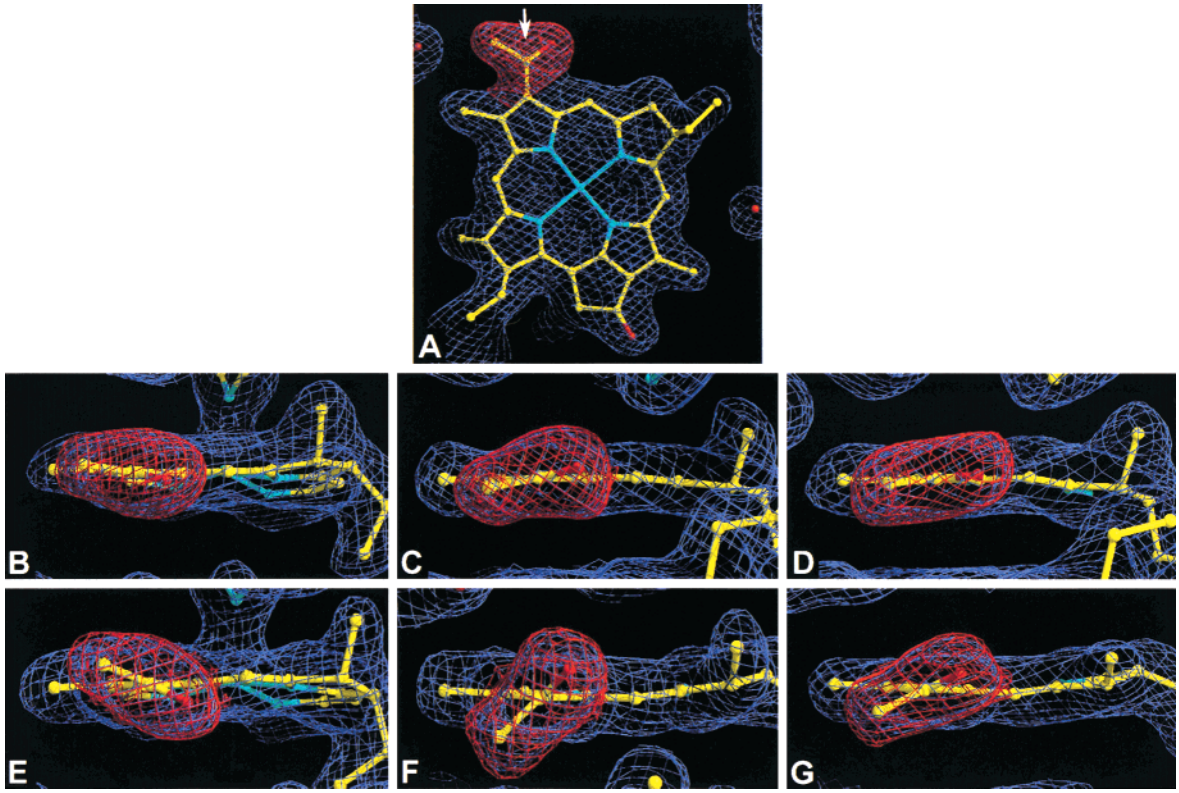

FIGURE 5: Electron density maps of the reaction center bacteriochlorins. (A) REFMAC $2mF_o - DF_c$ electron density map of the P_L BChl with the fitted structure of BChl. The 2-acetyl carbonyl group is at the top right, and the density attributed to this group is highlighted in red. (B−G) REFMAC $2mF_o - DF_c$ electron density maps and fitted structures showing a view of the 2-acetyl carbonyl group of each BChl (highlighted in red) down the axis of the C2−C2a bond (arrow in panel A), with the C1a methyl group on the left in each case. Data shown are (B) B_M BChl, (C) P_L BChl, (D) P_M BChl, (E) B_L BChl, (F) H_M BPhe, and (G) H_L BPhe.

transfer from P* to H_L. The crystallographic data presented above show that the Q_A ubiquinone is not present in the AM260W reaction center, which accounts for the lack of electron transfer from H_L to Q_A and the inability to generate millisecond time-scale charge-separated states such as $P^+Q_A^-$ or $P^+Q_B^-$ in this mutant (*18*).

The failure of this complex to bind the Q_A ubiquinone is presumably due to the presence of the Trp M260 residue, which occupies approximately one-half of the volume normally occupied by the headgroup of the Q_A ubiquinone. The other significant structural changes are the movement of residue Phe M258 to occupy space normally occupied by the tail of the Q_A ubiquinone and the incorporation of an ion, assigned as a chloride, which not only helps to fill the Q_A binding pocket but also may satisfy bonding requirements for neighboring polar groups. Repacking of the protein mainly concerns a short, nonhelical stretch of six amino acids, and the structural changes do not appear to have any significant effect on the structure or interactions of the nonheme iron (other than a slight change in the tilt of the His M190 residue, which provides one of the ligands to the iron) or the structure of the Q_B site.

Occupancy of the Q_B Site. The most surprising aspect of this study was the well-defined electron density obtained for the Q_B ubiquinone. As described in the Results, in previous studies we have found that electron density in the Q_B pocket is difficult to model, and this has been attributed to a combination of low occupancy of the pocket by ubiquinone, the possibility of multiple binding conformations for the ubiquinone, and the possibility of water molecules in the pocket depending on conformation/presence of the ubiquinone. In the present study, the well-defined electron density for the Q_B ubiquinone (Figure 3B) is ascribed to a higher-than-usual occupancy of the Q_B pocket by ubiquinone in the crystals of the AM260W reaction center. No particular steps were taken to achieve this, the isolation, purification, and crystallization procedures used for the AM260W reaction center being largely the same as those used in previous studies. The principal differences in the present study were the use of sodium citrate as the precipitant during crystallization and the relatively short time required for data acquisition. As described above, there was no indication of any changes in the structure of the Q_B pocket that could account for a tighter binding of ubiquinone in the AM260W reaction center.

The most likely explanation for the high occupancy of the Q_B site in the crystallized AM260W reaction center lies in the nature of the mutant complex. The standard procedure for depletion of Q_B ubiquinone involves illumination of the reaction center in the presence of a species that can reduce the photooxidized primary donor, which leads to the accumulation of doubly reduced and protonated ubiquinone (ubiquinol) at the Q_B site and release of this ubiquinol from the complex. Clearly, in the AM260W reaction center, this process is blocked due to the absence of the Q_A ubiquinone, which prevents light-driven reduction of Q_B by P (*18*). Our conclusion, therefore, is that unlike in functional reaction centers, the Q_B ubiquinone in the AM260W reaction center does not become reduced during the procedures involved in isolation, purification, and crystallization of the complex. As a result, occupancy of the Q_B pocket in the final crystallized form of the reaction center is relatively high. However, it

should be noted that the redox state of the Q_B ubiquinone was not monitored during the collection of X-ray data, and hence, at this stage, we cannot be certain as to the reduction/protonation state of the quinone shown in Figure 3B under these conditions.

Ubiquinone Conformation at the Q_B Site. The Q_B ubiquinone displays the most complex redox chemistry of all of the reaction center cofactors, undergoing a double reduction that is linked to the uptake of two protons. The ubiquinone can exist in three principal forms, unreduced ubiquinone, singly reduced semiquinone, and doubly reduced and protonated ubiquinol. Depending on the precise sequence of reduction and protonation reactions, additional intermediates are also possible during the conversion of semiquinone to ubiquinol. Two recent studies have used X-ray crystallography to examine the structure of the Q_B site and have addressed the question of how details of the structure can explain the sequence of reduction-coupled protonation reactions required to achieve conversion of ubiquinone to ubiquinol.

Stowell and co-workers (*50*) have examined the structural changes that accompany charge separation by comparing the structure of the *Rb. sphaeroides* R26 reaction center cooled to cryogenic temperatures under illumination with the structure of the complex cooled to cryogenic temperature in the dark. The results of this study were combined with the results of a spectroscopic study of the reaction center to produce a mechanism for light-driven reduction of Q_B based on conformational gating (*51*). The crystallized reaction centers had a Q_B occupancy of 60−70%, and this was increased further by soaking crystals in ubiquinone-2, a short chain analogue of the native ubiquinone-10 (*50*). Crystals cooled in the dark were estimated to be >95% in the neutral state, PQ_AQ_B, and generated a structural model at 2.2 Å resolution that was termed the dark structure. Crystals cooled under illumination were estimated to be ~90% in the charge-separated state, $P^+Q_AQ_B^-$, and generated a structural model at 2.6 Å resolution that was termed the light structure.

The principal difference between the two structures was in the conformation of the Q_B ubiquinone. In the light structure, the headgroup of the semiquinone was located deep in the Q_B pocket (termed the "light conformation"). The O4 carbonyl oxygen was hydrogen bonded to His L190, the O1 carbonyl oxygen was hydrogen bonded to the backbone amide nitrogen of Ile L224, and the O1 carbonyl oxygen was in a position to form a weak hydrogen bond with the side-chain hydroxyl of Ser L223 and the backbone amide nitrogen of Gly L225. In the dark structure, the headgroup of the ubiquinone was located closer to the entrance of the Q_B pocket (termed the "dark conformation"). The O4 carbonyl oxygen of the Q_B ubiquinone was hydrogen bonded to the backbone amide of Ile L224, and the O1 carbonyl oxygen was free from hydrogen bond interactions. In the dark structure, density was also observed in the Q_B pocket that could indicate a minor population of ubiquinones in the light conformation, or occupancy of that part of the pocket by water molecules. The change in structure on going from the dark to light conformation not only required a 4.5 Å movement of the ubiquinone headgroup deeper into the Q_B pocket but also required a 180° rotation of the headgroup of the ubiquinone. In the conformational gating mechanism, the rate of electron transfer from Q_A to Q_B was proposed to be limited by the rate of this conversion of the reaction center from the dark (inactive) conformation to the light (active) conformation and a number of possible factors that could control the rate of this gating process were discussed (*51*).

A study by Lancaster and Michel on the *Rps. viridis* reaction center has also addressed the question of changes in Q_B conformation during turnover of the reaction center (*41*). This study involved the crystallization of reaction centers depleted in ubiquinone, reaction centers reconstituted with ubiquinone-2, reaction centers inhibited at the Q_B site with stigmatellin, and the construction of structural models at 2.4−2.45 Å resolution. The outcome of this study was a mechanistic model of Q_B site turnover based around two basic binding conformations for the Q_B ubiquinone, a distal conformation in which the O4 carbonyl oxygen accepts a hydrogen bond from the backbone amide of Ile L224 and a proximal conformation in which the O4 carbonyl oxygen is hydrogen-bonded to His L190, and the O1 carbonyl oxygen forms two hydrogen bonds, one with the backbone amide nitrogen of Ile L224 and the other with the backbone amide nitrogen of Gly L225. The model envisages binding of ubiquinone in the distal conformation, followed by translation and a 180° rotation of the ubiquinone headgroup into the proximal conformation. Double reduction and protonation of the ubiquinone is then followed by exit of ubiquinol from the pocket, the resulting cavity being filled by water molecules.

The conformation adopted by native ubiquinone-10 in the structure of the AM260W reaction center is similar to the light conformation assigned to semiquinone in the light structure of Stowell and co-workers (*50*) and the proximal conformation described in the work of Lancaster and Michel (*41*). The three models are similar in that they all indicate a hydrogen bond between the O4 oxygen of the ubiquinone and the side-chain nitrogen of His L190, with a distance of 2.6 Å between the two. At the O1 oxygen of the ubiquinone, Stowell and co-workers described a hydrogen bond interaction with the backbone amide of Ile L224 (3.0 Å) and two possible weaker hydrogen bonds with the backbone amide of Gly L225 (3.3 Å) and the hydroxyl of Ser L223 (3.2 Å). Lancaster and Michel, on the other hand, described two hydrogen bond interactions with the backbone amides of Ile L224 (3.0 Å) and Gly L225 (2.9 Å) in the structure of the *Rps. viridis* reaction center reconstituted with ubiquinone-2, despite the fact that the hydroxyl of Ser L223 is in a suitable hydrogen-bonding position, 2.8 Å from the O4 carbonyl oxygen. Instead, an interaction of the hydroxyl of Ser L223 with the side-chain oxygen of Asn L213 was favored (2.8 Å) based on related studies on mutant complexes.

In the present study, the modeled structure in the vicinity of the O4 oxygen of the ubiquinone showed greater similarity to that of Lancaster and Michel than to that of Stowell and co-workers, with two possible hydrogen bond interactions between the O4 oxygen and the backbone amides of Ile L224 (3.0 Å) and Gly L225 (3.2 Å) and a third slightly shorter range interaction with the hydroxyl of Ser L223 (2.7 Å), which in turn was 2.6 Å from Asp (in *Rb. sphaeroides*) L213. One possible explanation for this variation could be that Ser L223 makes a slightly closer approach to the ubiquinone headgroup when the latter is in the ubiquinone state than when it is in the semiquinone state, as in the structure of Stowell and co-workers. However, although correctly un-

derstanding the pattern of hydrogen bond interactions in this area of the protein is of crucial importance if the detailed mechanism of coupled reduction and protonation of the Q_B ubiquinone is to be determined, it has to be remembered that the coordinate error in all of the structures discussed above is of the order of 0.3 Å and so small variations between independently determined structures have to be treated with some caution. In addition, as indicated above, the reduction/protonation state of the Q_B ubiquinone in the crystals of the AM260W reaction center was not monitored. As a result, we cannot rule out the possibility that it was in the semiquinone form during the collection of X-ray data, although we feel that the lack of the conventional route for the reduction of the Q_B ubiquinone makes this unlikely. At present, therefore, all that can be said with certainty is that all three structures show the same general features, with a single, strong hydrogen bond to the O1 oxygen of the ubiquinone headgroup and the possibility of multiple hydrogen bonds to the O4 oxygen.

It is apparent from our results that in the AM260W reaction center, where the occupancy of the Q_B pocket is high, the proximal/light conformation is favored for the binding of ubiquinone-10, with no evidence for a mixture of binding conformations. In that respect, our results are similar to those of Lancaster and Michel on *Rps. viridis* reaction centers reconstituted with ubiquinone-2 but differ from the dark structure of Stowell and co-workers, which was obtained with reaction centers containing a mixture of native ubiquinone-10 and ubiquinone-2 and where the ubiquinone was either all in the dark position or in a mixture of light and dark positions. Our findings therefore seem to rule out the possibility that in these structures the ubiquinone seen to be occupying the proximal/light position is the ubiquinone-2 used in reconstitutions, while the ubiquinone seen to be occupying the distal/dark position is the native ubiquinone-10. Were this to be the case, then all of the Q_B ubiquinone in the AM260W reaction center would be expected to occupy the distal position, in contrast to the experimental results.

Carotenoid Conformation and Binding by the Reaction Center. Not all of the structures of the *Rb. sphaeroides* reaction center deposited in the Protein Data Bank include the single reaction center carotenoid. This is due to the use of the carotenoidless R26 strain as a source of reaction centers in some studies. Where it is present, there is considerable variation in the detailed conformation of the reaction center carotenoid, reflecting the difficulty in accurately modeling this particular cofactor (*4*, *5*, *42*−*45*). In some of the structures deposited in the Protein Data Bank, the carotenoid has been modeled with a 13,14-cis conformation (*4*, *5*, *42*). The high-quality electron density maps obtained in the present study have allowed us to model the reaction center carotenoid with some confidence, and in particular, as illustrated in Figure 4, the electron density is best modeled by a carotenoid with a 15−15′ cis conformation, in line with long-standing conclusions based on spectroscopic studies (*46*, *47*).

The modeled conformation of the Trp M75 residue in the present study, with the indole nitrogen pointing toward the end of the carotenoid, is similar to the conformation modeled in the 1PST and 1PSS structures of Chirino and co-workers (*42*) and in the 1YST structure of Arnoux and co-workers (*44*). However, in terms of the orientation of the terminal methoxy group, the structural model of the carotenoid in the AM260W reaction center is different from those in the 1PST, 1PSS, and 1YST structures. The conformation of the methoxy group in the present study was similar to that described in the 1PCR structure by Ermler and co-workers (*4*, *5*), but in the 1PCR structure the Trp M75 residue is modeled in a conformation that would not allow a hydrogen bond interaction with the methoxy group of the carotenoid. In the present study, the conformations of Trp M75 and the spheroidenone methoxy group that gave the best fits to the electron density (Figure 4C) placed the indole nitrogen and methoxy oxygen in orientations that strongly suggested a hydrogen bond interaction between the two (separation 3.1 Å). It should be commented that essentially the same interaction was apparent in the structural model of the FM197R/YM177F reaction center described by us recently (*23*) and deposited in the Protein Data Bank under the code 1MPS. The same is also true for structures of the wild-type (*23*) and FM197R/WM115F reaction centers determined by our group (*35*). However, we have not commented on this probable carotenoid−protein interaction in previous reports because the precise conformation of the spheroidenone was less clear in previous structures due to the lower quality of the electron density maps.

In the present study, we have modeled the reaction center carotenoid as spheroidenone, as in all our studies *Rb. sphaeroides* cells are grown under semiaerobic conditions in the dark. However, it seems likely that the carotenoid−protein interaction described above would be retained in reaction centers in photosynthetically grown cells, as spheroidene (the carotenoid formed under such conditions) retains the terminal methoxy group, differing from spheroidenone only in the lack of the carbonyl group at carbon 2 of the polyene chain (which does not interact with the surrounding protein; see above). However, an interaction with the protein involving a noncovalent bond is probably not essential for carotenoid binding by the reaction center per se, as 1,2-dihydroneurosporene, a green carotenoid found in the *Rps. viridis* reaction center, does not have the terminal methoxy group (or any oxy groups for that matter). Interestingly, residue Trp M75 is not conserved in the *Rps. viridis* reaction center, being replaced by alanine.

A large number of mutants of *Rb. sphaeroides* have been isolated that have green carotenoids such as neurosporene and its oxygenated derivatives, rather than the red/brown spheroidene/spheroidenone. It has been noted, however, that the *Rb. sphaeroides* reaction center preferentially binds methoxy and hydroxy carotenoids, such as spheroidene/spheroidenone and methoxyneurosporene, rather than non-oxygenated carotenoids such as neurosporene (*8*, *52*). The hydrogen bond donated by Trp M75 could provide an explanation for this preference and perhaps for more subtle effects, such as an apparent preference of the *Rb. sphaeroides* reaction center for spheroidenone over spheroidene, which may be related to the fine detail of the carotenoid−Trp interaction.

Influence of the 2-Acetyl Carbonyl Groups on the Optical and Electronic Properties of the Reaction Center Bacteriochlorins. A number of computational studies have predicted that the optical properties of the reaction center BChls and BPhes should be influenced by the orientation of the 2-acetyl

group relative to the plane of the macrocycle (*53*−*55*). It is also to be expected that the electrochemical properties of these bacteriochlorins will be affected by the orientation of the acetyl group (*49*). In the present study, the quality of the electron density maps has allowed us to judge with reasonable accuracy the angle made by the acetyl group relative to the bacteriochlorin ring and also to make proposals concerning which "arms" of the electron density correspond to the methyl and carbonyl groups (Figure 5).

A striking observation that is depicted in Figure 5 is that, regardless of tilt, the assigned overall orientation is the same in all six cases in that the methyl arm of the acetyl group is nearest to the methyl group 1a that is attached to carbon 1 of ring I. This may be fortuitous or represent a preferred conformation. However, it is worth repeating that even at a resolution of 2.1 Å it is not possible to be absolutely certain as to which arm of the acetyl group is the methyl and which is the carbonyl oxygen, and so at present the assignments shown have to be regarded as proposals of the most probable conformations.

As explained in the Results, the orientation of the 2-acetyl carbonyl group can be quantitated in terms of the C12−C2−C2a−O dihedral angle ϕ_{Ac}. Molecular orbital calculations of the RHF-INDO/SP type have revealed that the total energy of BChl $a^{\bullet+}$ and BPhe $a^{\bullet-}$ in vacuo as a function of ϕ_{Ac} has two minima at $\phi_{Ac} \approx 45°$ and $\phi_{Ac} \approx 135°$, separated by a small barrier at $\phi_{Ac} \approx 90°$ (*56*, *57*). The total energy rises strongly when ϕ_{Ac} approaches 0° or 180°, because of steric hindrance. Only the H_M BPhe shows a conformation that might conform to such an energy minimum (Figure 5F), with $\phi_{Ac} = 43°$. The remaining bacteriochlorins have a ϕ_{Ac} that is between 28° and −27°.

Comparisons of the modeled conformation of the bacteriochlorin acetyl groups in the various structures for the *Rb. sphaeroides* reaction center deposited in the Protein Data Bank show that, for each of the bacteriochlorins, the gross conformation of the acetyl group is similar. In general, the acetyl groups of the BChl cofactors show an approximately in-plane geometry, while the acetyl groups of the BPhe cofactors show a more out-of-plane geometry (as illustrated in Figure 5). For each bacteriochlorin, there is some variation in the precise geometry of the acetyl group relative to the plane of the bacteriochlorin ring and in the assignment of the methyl and carbonyl arms of the group, but this is no more than the variation that would be expected among structures based on data obtained at different resolutions (between 2.2 and 3.1 Å) and on electron density maps of varying quality. The most notable exception to this gross consensus is the orientation of the acetyl carbonyl of the P_L BChl in the 1PCR structure of Ermler and co-workers (*4*, *5*), which is modeled with an approximately 90° out-of-plane geometry. This is of interest because it is the only acetyl group of the six reaction center bacteriochlorins that is hydrogen-bonded to the surrounding protein, the hydrogen bond being donated by the residue of His L168. In the structure of the AM260W reaction center, the assignment of the methyl and carbonyl arms of the P_L acetyl group (Figure 5C) is consistent with the presence of a hydrogen bond interaction with His L168. The carbonyl group points toward His L168, with a separation of 2.9 Å between the carbonyl oxygen and the NE2 nitrogen of His L168. However, the ϕ_{Ac} of 13° reported for the acetyl of the P_L BChl in the present study is clearly at odds with the approximately 90° out-of-plane geometry described by the 1PCR structure. The orientation of this group in the structure of the AM260W reaction center is more consistent with the orientations of this group in the remaining structures available in the Protein Data Bank and with a number of structures for mutant *Rb. sphaeroides* reaction centers determined by our group (*23*, *35*−*37*).

Conformational Freedom of the 2-Acetyl Carbonyl Group. An intriguing question concerns whether the orientation of one or more of the acetyl groups of the reaction center bacteriochlorins changes during or following light-driven electron transfer. In the wild-type reaction center, absorption of a photon by P triggers the stepwise transfer of an electron across the membrane. The electron is transferred from P to B_L in 3−5 ps, from B_L to H_L in 1−2 ps, and from H_L to Q_A in 200 ps, each step being accompanied by characteristic changes in the absorption properties of the complex (*6*, *7*). These changes are due to the bleaching of ground state absorbance bands, anion and cation absorbance, excited state absorbance and emission, and shifts in absorbance bands due to the electric field created as the positive and negative charges are separated by the electron transfer process. The nature of any conformational changes in the cofactor−protein matrix that occur in response to the movement of the electron is only poorly understood, but one of the most obvious ways in which the bacteriochlorins can respond to changes in their environment is through rotation of the 2-acetyl group. Presumably, the conformation of each 2-acetyl group in the reaction center represents an energy minimum that is determined by the interaction of the acetyl group with the rest of the bacteriochlorin ring and the surrounding protein. If this energy minimum changes when the redox state of the bacteriochlorin is altered or if it changes in response to a change in the structure of the protein, then rotation of the acetyl group may occur, with the possibility of accompanying changes in the absorption spectrum of the bacteriochlorin, as described above.

It has been proposed recently on the basis of ^{1}H-Special TRIPLE spectroscopy that the 2-acetyl carbonyl group of the H_L anion can adopt more than one conformation in freeze trapped *Rb. sphaeroides* reaction centers, termed H_{L1}^- and H_{L2}^- (*58*, *59*). The relevance of these conformations to relaxation processes and the energetics of primary electron transfer have been discussed (*58*−*60*). It was suggested that the H_{L1}^- state, with $\phi_{Ac} = 45°$ or 315° (i.e., −45°), and the H_{L2}^- state, with $\phi_{Ac} = 135°$ or 225° (i.e. −135°), reflected different conformations of H_L^- associated with different redox states of the reaction center. In the present study, H_L had $\phi_{Ac} = 28°$, which would be broadly consistent with the proposed orientation of the acetyl group in the H_{L1}^- state. However, as discussed above, we cannot rule out the possibility that H_L had $\phi_{Ac} = 208°$ in our study, which would be more consistent with the proposed orientation of the group in the H_{L2}^- state. We are currently attempting to obtain higher resolution X-ray data to address this point further.

SUPPORTING INFORMATION AVAILABLE

Comparisons of the positions of the C_α carbons of the M polypeptide in the structural models of the AM260W and

RCO2 reaction centers. This information is available free of charge via the Internet at http://pubs.acs.org.

REFERENCES

1. Allen, J. P., Feher, G., Yeates, T. O., Komiya, H., and Rees, D. C. (1987) *Proc. Natl. Acad. Sci. U.S.A. 84*, 5730−5734.
2. Komiya, H., Yeates, T. O., Rees, D. C., Allen, J. P., and Feher, G. (1988) *Proc. Natl. Acad. Sci. U.S.A. 85*, 9012−9016.
3. Chang, C.-H., El-Kabbani, O., Tiede, D., Norris, J., and Schiffer, M. (1991) *Biochemistry 30*, 5352−5360.
4. Ermler, U., Fritzsch, G., Buchanan, S. K., and Michel, H. (1994) *Structure 2*, 925−936.
5. Ermler, U., Michel, H., and Schiffer, M. (1994) *J. Bioenerg. Biomembr. 26*, 5−15.
6. Fleming, G. R., and van Grondelle, R. (1994) *Phys. Today 47*, 48−55.
7. Hoff, A. J., and Deisenhofer, J. (1997) *Phys. Rep. 287*, 1−247.
8. Cogdell, R. J., and Frank, H. A. (1987) *Biochim. Biophys. Acta 895*, 63−79.
9. Frank, H. A. (1993) in *The Photosynthetic Reaction Center* (Deisenhofer, J., and Norris, J. R., Eds.) Vol. 2, pp 221−239. Academic Press, San Diego.
10. Frank, H. A., and Cogdell, R. J. (1993) in *Carotenoids in Photosynthesis* (Young, A. J., and Britton, G., Eds.), pp 252−326, Chapman and Hall, London.
11. Deisenhofer, J., Epp, O., Miki, K., Huber, R., and Michel, H. (1985) *Nature 318*, 618−624.
12. Deisenhofer, J., Epp, O., Sinning, I., and Michel, H. (1995) *J. Mol. Biol. 246*, 429−457.
13. Allen, J. P., Feher, G., Yeates, T. O., Rees, D. C., Deisenhofer, J., Michel, H., and Huber, R. (1986) *Proc. Natl. Acad. Sci. U.S.A. 83*, 8589−8593.
14. Coleman, W. J., and Youvan, D. C. (1990) *Annu. Rev. Biophys. Biophys. Chem. 19*, 333−367.
15. Woodbury, N. W., and Allen, J. P. (1995) in *Anoxygenic Photosynthetic Bacteria* (Blankenship, R. E., Madigan, M. T., and Bauer, C. E., Eds.), pp 527−557, Kluwer Academic Publishers, The Netherlands.
16. Okamura, M. Y., and Feher, G. (1995) in *Anoxygenic Photosynthetic Bacteria* (Blankenship, R. E., Madigan, M. T., and Bauer, C. E., Eds.), pp 577−594, Kluwer Academic Publishers, The Netherlands.
17. Fyfe, P. K., McAuley-Hecht, K. E., Jones, M. R., and Cogdell, R. J. (1998) in *Biomembrane Structures* (Haris, P. I., and Chapman, D., Eds.), pp 64−87, IOS Press, Amsterdam, The Netherlands.
18. Ridge, J. P., van Brederode, M. E., Goodwin, M. G., van Grondelle, R., and Jones, M. R. (1999) *Photosynth. Res. 59*, 9−26.
19. McAuley, K. E., Fyfe, P. K., Ridge, J. P., Isaacs, N. W., Cogdell, R. J., and Jones, M. R. (1999) *Proc. Natl. Acad. Sci. U.S.A. 96*, 14706−14711.
20. Jones, M. R., Fowler, G. J. S., Gibson, L. C. D., Grief, G. G., Olsen, J. D., Crielaard, W., and Hunter, C. N. (1992) *Mol. Microbiol. 6*, 1173−1184.
21. Jones, M. R., Visschers, R. W., van Grondelle, R., and Hunter, C. N. (1992) *Biochemistry 31*, 4458−4465.
22. Jones, M. R., Heer-Dawson, M., Mattioli, T. A., Hunter, C. N., and Robert, B. (1994) *FEBS Lett. 339*, 18−24.
23. McAuley-Hecht, K. E., Fyfe, P. K., Ridge, J. P., Prince, S. M., Hunter, C. N., Isaacs, N. W., Cogdell, R. J., and Jones, M. R. (1998) *Biochemistry 37*, 4740−4750.
24. Buchanan, S. K., Fritzsch, G., Ermler, U., and Michel, H. (1993) *J. Mol. Biol. 230*, 1311−1314.
25. Otwinowski, Z., and Minor, W. (1997) *Methods Enzymol. 276*, 307−326.
26. Brünger, A. T., Juriyan, J., and Karplus, M. (1987) *Science 235*, 458−460.
27. Murshudov, G. N., Vagin, A. A., and Dodson, E. J. (1997) *Acta Crystallogr. D53*, 240−255.
28. Lamzin, V. S., and Wilson, K. S. (1993) *Acta Crystallogr. D49*, 129−147.
29. Engh, R. A., and Huber, R. (1991) *Acta Crystallogr. A47*, 392−400.
30. Allen, F. H., Bellard, S., Brice, M. D., Cartwright, B. A., Doubleday, A., Higgs, H., Hummelink, Th., Hummelink-Peters, B. G., Kennard, O., Motherwell, W. D. S., Rodgers, J. R., and Watson, D. G. (1979) *Acta Crystallogr. B35*, 2331−2339.
31. Kraulis, P. J. (1991) *J. Appl. Crystallogr. 24*, 946−950.
32. Merritt E. A., and Bacon, D. J. (1997) *Methods Enzymol. 277*, 505−524.
33. McRee, D. E. (1992) *J. Mol. Graphics 10*, 44−46.
34. Collaborative Computational Project No. 4. (1994) *Acta Crystallogr., D50*, 760−763.
35. Ridge, J. P., Fyfe, P. K., McAuley, K. E., van Brederode, M. E., Robert, B., van Grondelle, R. Isaacs, N. W., Cogdell, R. J., and Jones, M. R. *Biochem. J.*, in press.
36. McAuley, K. E., Fyfe, P. K., Cogdell, R. J., Isaacs, N. W., and Jones, M. R. (2000) *FEBS Lett. 467*, 285−290.
37. Fyfe, P. K., Ridge, J. P., McAuley, K. E., Cogdell R. J., Isaacs, N. W., and Jones, M. R. (2000) *Biochemistry*, *39*, 5953−5960.
38. El-Kabbani, O., Chang, C. H., Tiede, D., Norris, J., and Schiffer, M. (1991) *Biochemistry*, *30*, 5361−5369.
39. Allen, J. P., Feher, G., Yeates, T. O., Komiya, H., and Rees, D. C. (1988) *Proc. Natl. Acad. Sci. U.S.A. 85*, 8497−8491.
40. Stowell, M. H. B., McPhillips, T. M., Rees, D. C., Soltis, S. M., Abresch, E., and Feher, G. (1997) *Science*, *276*, 812−816.
41. Lancaster, C. R. D., and Michel, H. (1997) *Structure 5*, 1339−1359.
42. Chirino, A. J., Lous, E. J., Huber, M., Allen, J. P., Schenck, C. C., Paddock, M. L., Feher, G., and Rees, D. C. (1994) *Biochemistry 33*, 4584−4593.
43. Arnoux, B., Ducruix, A., Reiss-Husson, F., Lutz, M., Norris, J., Schiffer, M., and Chang, C.-H. (1989) *FEBS Lett. 258*, 47−50.
44. Arnoux, B., Gaucher, J.-F., Ducruix, A., and Reiss-Husson, F. (1995) *Acta Crystallogr. D51*, 368−79.
45. Yeates, T. O., Komiya, H., Chirino, A., Rees, D. C., Allen, J. P., and Feher, G. (1988) *Proc. Natl. Acad. Sci. U.S.A. 85*, 7993−7997.
46. Koyama, Y., Takii, T., Saiki, K., Tsukida, K., and Yamashita, K. J. (1982) *Biochim. Biophys. Acta*, *680*, 109−118.
47. Lutz, M., Szponarski, W., Berger, G., Robert, B., and Neuman, J. (1987) *Biochim. Biophys. Acta 894*, 423−433.
48. Lancaster, C. R. D., and Michel, H. (1999) *J. Mol. Biol. 286*, 883−898.
49. Hanson, K. L. (1991) in *Chlorophylls* (Scheer, H., Ed.), pp 993−1014, CRC Press, Boca Raton, FL.
50. Stowell, M. H. B., McPhillips, T. M., Rees, D. C., Soltis, S. M., Abresch, E., and Feher, G. (1997) *Science 276*, 812−816.
51. Graige, M. S., Feher, G., and Okamura, M. Y. (1998) *Proc. Natl. Acad. Sci. U.S.A. 95*, 11679−11684.
52. Chadwick, B. W., and Frank, H. A. (1986) *Biochim. Biophys. Acta 851*, 257−266.
53. Parson, W. W., and Warshel, A. (1987) *J. Am. Chem. Soc. 109*, 6152−6163.
54. Gudowska-Nowak, E., Newton, M. D., and Fajer, J. (1990) *J. Phys. Chem. 94*, 5795−5801.
55. Thompson, M. A., Zerner, M. C., and Fajer, J. (1991) *J. Phys. Chem. 95*, 5693−5700.
56. Plato, M., Möbius, K., and Lubitz, W. (1991) in *Chlorophylls* (Scheer, H., Ed.), pp 1015−1046, CRC Press, Boca Raton, FL.
57. Käss, H., Rautter, J., Zweygart, W., Struck, A., Scheer, H., and Lubitz, W. (1994) *J. Phys. Chem. 98*, 354−363.
58. Müh, F., Jones, M. R., and Lubitz, W. L. (1999) *Biospectroscopy 5*, 35−46.
59. Müh, F., Williams, J. C., Allen, J. P., and Lubitz, W. L. (1998) *Biochemistry 37*, 13066−13074.
60. Breton, J., Bibikova, M., Oesterhelt, D., and Nabedryk, E. (1999) *Biochemistry 38*, 11541−11552.
61. Brünger, A. T. (1992) *Nature 335*, 472−475.
62. Laskowski, R. A., MacArthur, W. W., Moss, D. S., and Thornton, J. M. (1993) *J. Appl. Crystallogr. 26*, 283−291.
63. Cruickshank, D. W. J. (1999) *Acta Crystallogr., Sect. D 55*, 583−601.

BI000557R